

1 **An X-ray photoelectron spectroscopic perspective for the evolution of O-**  
2 **containing structures in char during gasification**

3

4

5 Shuai Wang, Liping Wu, Xun Hu, Lei Zhang, Kane M O'Donnell, Craig E Buckley  
6 and Chun-Zhu Li\*

7

8

9 Fuels and Energy Technology Institute, Curtin University of Technology, GPO Box  
10 U1987, Perth, WA 6845, Australia

11

12

Submitted to

13

Fuel Processing Technology

14

For consideration for publication

15

16

Oct 2017

17

18

19 \*Corresponding author: [chun-zhu.li@curtin.edu.au](mailto:chun-zhu.li@curtin.edu.au); telephone: +61 8 9266 1131;

20 facsimile: +61 8 9266 1138

21 **Abstract**

22

23 The purpose of this study is to investigate the evolution of O-containing structures of  
24 char during gasification. Mallee wood (4.75-5.60 mm) from Western Australia was  
25 gasified in a fluidised-bed reactor at 600-900 °C in O-containing (pure CO<sub>2</sub>, 15%  
26 H<sub>2</sub>O-Ar) and non-O-containing atmospheres (15% H<sub>2</sub>-Ar). X-ray photoelectron  
27 spectroscopy (XPS) was applied to obtain detailed information about the nature of  
28 oxygen bonding with carbon as well as the content of oxygen species in char. The  
29 similar O/C ratio of char from XPS and elemental analysis indicated the relative  
30 chemical uniformity between char surface and char matrix. The deconvolution results  
31 of the O 1s spectra showed that the reactivity of the inherent aromatic C-O structure  
32 was much higher than that of the aromatic C=O structure during gasification. The  
33 amount of aromatic C-O structure left in char during gasification in non-O-containing  
34 atmosphere was lower than that in O-containing atmosphere while the consumption  
35 of aromatic C=O structure was proportional to the progress of gasification,  
36 regardless of the atmosphere. The newly formed C-O structure in char during the  
37 gasification in the O-containing atmosphere was likely to be responsible for the high  
38 gasification reactivity. The well-dispersed alkali earth metallic species could be  
39 carbonated to form CaCO<sub>3</sub> and MgCO<sub>3</sub> on char surface once the char was exposed  
40 to CO<sub>2</sub> at 900 °C.

41

42 **Keywords:** X-ray photoelectron spectroscopy; Oxygen-containing structure; Char  
43 oxygenation; Gasification; Biomass

44

45

## 46 **1. Introduction**

47

48 Char gasification is the rate-limiting step for the overall solid fuel gasification  
49 process [1,2]. There are a few important inter-related factors influencing the char  
50 gasification rate [3]. Firstly, the inherent alkali and alkaline earth metallic (AAEM)  
51 species in char can act as excellent catalysts for char gasification [3]. The presence  
52 of highly dispersed AAEM species can significantly speed up the gasification  
53 reaction, affect the properties of pyrolysis products, and have a great impact on the  
54 evolution of the char structure [4-8]. Secondly, the transformation of aromatic ring  
55 systems in char will greatly influence char reactivity during gasification. It has  
56 become clear that the small ring systems (equivalent to 3-5 fused benzene rings) are  
57 preferentially consumed while the large ones (more than 6 fused rings) are  
58 preferentially left and/or formed during gasification, making the residual char more  
59 condensed and hard to gasify [9-13]. Thirdly, the O-containing functional groups in  
60 char will also greatly influence the gasification rate to some extent, especially for the  
61 gasification of the low-rank fuels at low temperature. It is believed that some O-  
62 containing structures in char are responsible for enhancing the char gasification rate  
63 [4,9]. For a better understanding of the gasification mechanisms, the changes in char  
64 structure, especially the evolution of O-containing structures, must be quantified  
65 during gasification.

66 FT-Raman spectroscopy has been demonstrated to be a powerful analytical  
67 method to characterise the evolution of aromatic ring systems in char during  
68 gasification due to its outstanding ability to respond to the non-polar bond vibration  
69 [14-20]. However, only limited information can be obtained from the Raman spectra  
70 about the changes of O-containing structures in char, especially the changes in the

71 chemical bonding between oxygen and carbon during gasification. The total Raman  
72 intensity can be used as an indication of the relative amount of the O-containing  
73 functional groups in char that can induce a resonance effect between oxygen and  
74 the aromatic ring to which it is connected [14]. Not all oxygen species in char could  
75 have the resonance effect with the aromatic rings. Fourier transform infrared (FT-IR)  
76 spectroscopy may be responsive to a wide range of O-containing structures in char.  
77 However, FT-IR spectroscopy would have some potential difficulties within the  
78 context of tracing the changes in the O-containing structures during gasification. For  
79 example, the absorption coefficients may vary by a magnitude or more from one type  
80 of O-containing functional group to another.

81 Therefore, other techniques must be applied to study O-containing functional  
82 groups in char and provide useful information on the evolution of O-containing  
83 structures in char during gasification. X-ray photoelectron spectroscopy (XPS) has  
84 proved to be one of the most powerful tools in detecting the surface structure of  
85 carbonaceous materials [21-24]. Although the validity of XPS analysis is limited to  
86 determining the surface structure of material, its high sensitivity to the chemical  
87 nature of atomic species has made it extensively developed as a useful technique for  
88 identifying the structural features of different types of carbon materials [25,26]. In  
89 addition, the ability to identify elemental bonding states has make it widely used in  
90 determining the organic functional group composition of char through a detailed  
91 analysis of the high-resolution band of each elements [27,28]. Another important  
92 feature of XPS spectroscopy is the unchanged sensitivity of oxygen regardless of its  
93 chemical structures/functionality. This greatly facilitates the relative quantification of  
94 various classes of O-containing structures simply based on the measured peak  
95 areas.

96 The purpose of this study is to investigate the effects of gasification temperature  
97 and gasification atmosphere on the evolution of O-containing structures in char. XPS  
98 has been applied to characterise oxygen species in chars produced from the  
99 gasification of mallee wood at 600-900 °C in three different atmospheres (pure CO<sub>2</sub>,  
100 15% H<sub>2</sub>O-Ar, 15% H<sub>2</sub>-Ar). The high-resolution O 1s peak of the XPS spectra were  
101 further deconvoluted in order to gain insights into the nature of the bonding between  
102 oxygen and carbon in addition to the determination of the contents of oxygen in char.  
103 Our data provided further insight into the char gasification mechanisms.

104

## 105 **2. Experimental**

106

### 107 *2.1 Biomass gasification*

108

109 Mallee wood in the size range of 4.75-5.60 mm from Western Australia was used  
110 as the feedstock in this research. The proximate analysis of the sample results in a  
111 0.9% ash yield and 81.6% volatiles yield, and the elemental analysis of the sample  
112 determined 48.2% C, 6.1% H, 0.2% N and 45.5% O (wt%, dry and ash-free basis).

113 A fluidised-bed quartz reactor [29] was used to carry out the biomass gasification  
114 experiments. Approximately 2 g of biomass (weighed accurately) was pre-loaded  
115 into the feeder. Before feeding, the reactor was heated to the target temperature with  
116 the flow of Ar through the reactor. The feeding of biomass into the reactor  
117 commenced with the help of an electrical vibrator. When the feeding was finished,  
118 the reactor was held for 20 minutes to ensure that all volatiles had been released.  
119 The reaction gas was switched from Ar to the gasifying agent. For gasification in the  
120 steam atmosphere, it was 15% steam balanced with Ar. For gasification in the H<sub>2</sub>  
121 atmosphere, it was 15% H<sub>2</sub> balanced with Ar. For gasification in the CO<sub>2</sub> atmosphere,

122 pure CO<sub>2</sub> was used. After 4 minutes of holding in the gasification atmosphere, the  
123 reactor was lifted out of the furnace and cooled down naturally with Ar flowing into  
124 the reactor instead of the gasifying agents. After each experiment, the collected char  
125 sample was placed in sealed vials and stored in a freezer to avoid further oxidation  
126 by the ambient oxygen.

127

## 128 *2.2 Char characterisation*

129

130 XPS spectra were acquired with a Kratos AXIS Ultra DLD XPS spectrometer  
131 equipped with a Al-K $\alpha$  X-ray monochromator (photon energy 1486.7 eV). XPS  
132 measurements were carried out under ultra-high vacuum conditions ( $< 2.0 \times 10^{-10}$   
133 mbar) at room temperature. The survey scans were taken across the sample with  
134 binding energy from 1400 to 0 eV to determine all elements present in char. A pass  
135 energy of 40 eV was used for the collection of high-resolution spectrum of each of  
136 the selected elements.

137 Elemental analysis was carried out using a FLASH 200 elemental analyser. Char  
138 sample was firstly ground to powder and then about 2.5 mg (weighed accurately)  
139 sample was loaded into a tin capsule. The tin capsule was folded and placed in the  
140 autosampler for analysis.

141

## 142 **3. Deconvolution and band assignment of the XPS spectra**

143

144 Data processing of the acquired XPS spectra of chars was performed using the  
145 CasaXPS peak fitting software. The binding energy of the original XPS spectra was  
146 calibrated with respect to the carbon component of the C 1s peak at 284.5 eV. The  
147 spectra were curve-fitted after linear pre-edge and Shirley background subtraction,

148 using mixed Gaussian-Lorentzian bands. The position and assignment of the bands  
149 in the O 1s spectra are briefly summarised in Table 1.

150

151 **Table 1** Summary of peak/band assignment.

| Spectra | Band position, eV | Description             | References  |
|---------|-------------------|-------------------------|-------------|
| O 1s    | 531.4             | Aromatic C=O structure  | 11,27,30-32 |
|         | 533.4             | Aromatic C-O structure  | 23,27,31-33 |
|         | 536.0             | Absorbed O <sub>2</sub> | 11,23       |

152

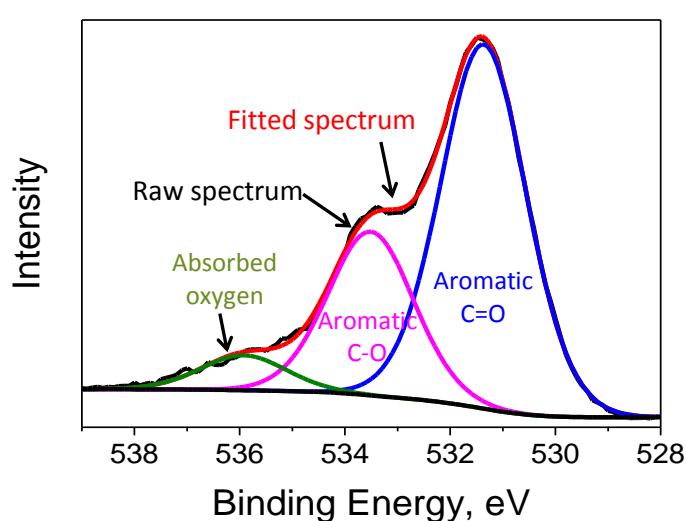
153 The curve-fitting of the high-resolution O 1s spectra was taken in the range  
154 between 528.0 and 539.0 eV. The broadening of the O 1s spectra means large  
155 varieties of O-containing structures presented in char. Based on the XPS spectra of  
156 some model compounds [11,30,31], one band at 531.3 eV was assigned to the C=O  
157 (aromatic) functional groups such as benzoquinone-type structure in char. Another  
158 band at 531.6 eV was attributed to the R-(C=O)-C (aromatic) functional groups such  
159 as aromatic ketone or carbonyl structure in char [27,31,32]. It is clear that these two  
160 kinds of O-containing functional groups have very close binding energies and they  
161 cannot be reliably distinguished through the curve-fitting procedure. Therefore, in this  
162 study, the band at 531.4 eV was assigned to all aromatic C=O structures in char.  
163 Since it represents more than one type of structure the band is broader than that for  
164 a pure model compound.

165 On the high binding energy side, one band at the position 533.2 eV was attributed  
166 to oxygen inside the carbon ring such as epoxide or furan type structure in char  
167 [27,31,33]. Another band at 533.3 eV was assigned to the O-C (aromatic) structure  
168 such as phenol or diphenyl ether [23,31,32]. Moreover, the band located at 533.6 eV  
169 was assigned to the O-(C=O)-C (aromatic) functional group such as carboxyl  
170 structure in char [31]. Similarly, because of the close binding energies among these

171 three oxygen-carbon structures and the complexity of O-containing functional groups  
172 in char, the band at 533.4 eV was assigned to all aromatic C-O structures in char.

173 In addition to the two main bands assigned above, another weak peak appearing  
174 at 536.0 eV was identified as the absorbed O<sub>2</sub> existing on char surface [11,23].

175 A typical example of the spectral deconvolution/curve-fitting of the high-resolution  
176 O 1s peak of char using three bands is shown in Fig. 1. Similar success of curve-  
177 fitting can also be achieved for all other char samples investigated in this study.



178  
179 **Fig. 1.** Spectral deconvolution of a XPS O 1s peak of char from the gasification of mallee wood at  
180 700 °C in 15% H<sub>2</sub>O balanced with Ar.

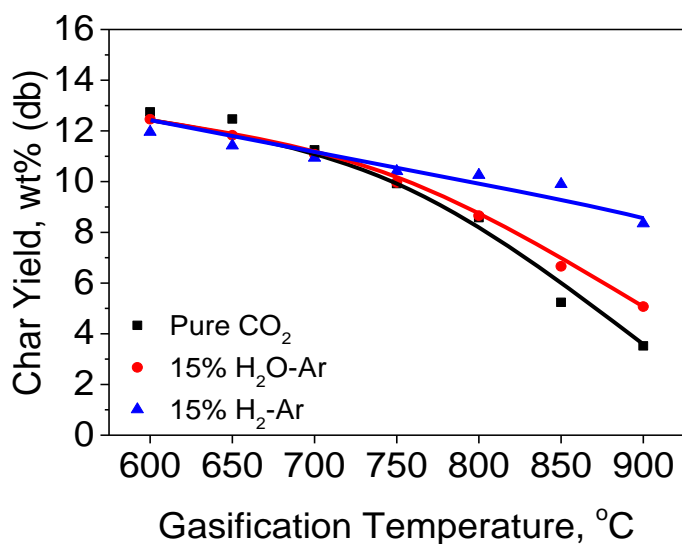
181  
182 **4. Results and discussion**

183  
184 **4.1 Char yield**

185  
186 The gasification of mallee woody biomass was carried out at different  
187 temperatures ranging from 600 to 900 °C in three gasifying agents (pure CO<sub>2</sub>, 15%  
188 H<sub>2</sub>O-Ar, 15% H<sub>2</sub>-Ar). Fig. 2 shows the char yields as a function of gasification  
189 temperature in three gasifying atmospheres. As expected, the char yield decreased



190 with increasing temperature because of the enhanced thermal cracking and  
191 gasification reaction. In addition, for different gasification atmospheres, when the  
192 temperature was below 700 °C, there was not much difference in the char yield,  
193 indicating that the main reaction was pyrolysis at this stage. However, when the  
194 temperature was higher than 700 °C, the gasification reaction became fierce and the  
195 gasification in CO<sub>2</sub> proceeded the fastest among the three atmospheres. As  
196 expected, the conversion of char proceeded the slowest during the gasification in H<sub>2</sub>  
197 atmosphere, confirming that the char-H<sub>2</sub> reaction was much slower than the char-  
198 H<sub>2</sub>O and char-CO<sub>2</sub> reactions [4,16].

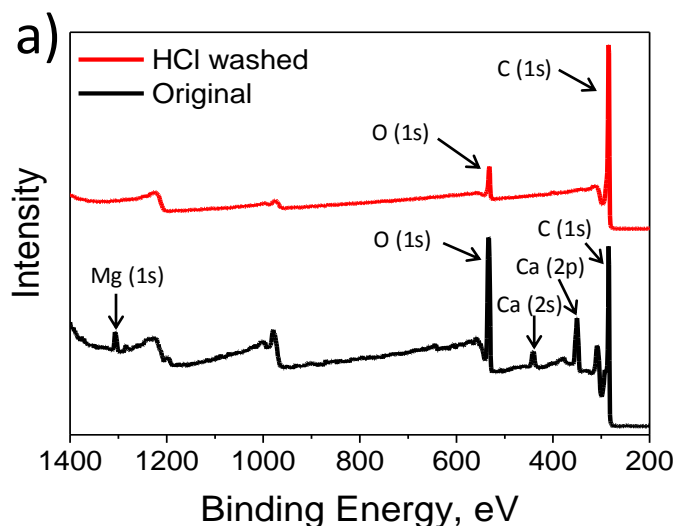


199  
200 **Fig. 2.** Char yield as a function of gasification temperature for mallee wood in pure CO<sub>2</sub>, 15% H<sub>2</sub>O  
201 balanced with Ar and 15% H<sub>2</sub> balanced with Ar.

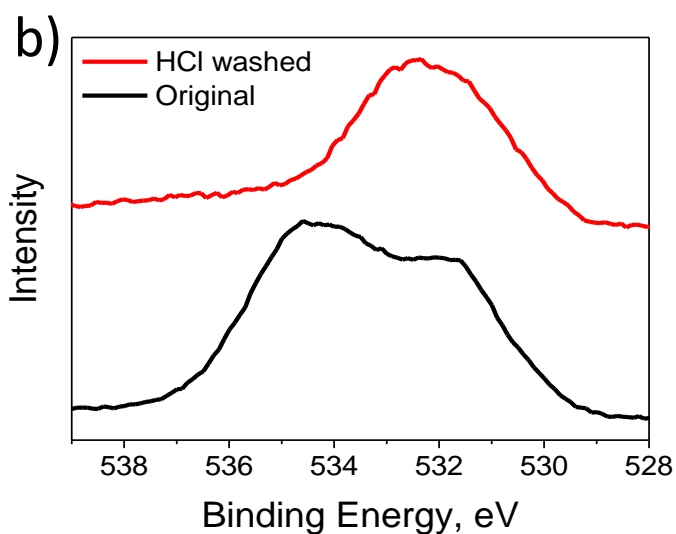
202  
203 *4.2 Formation of carbonates during the gasification in CO<sub>2</sub> at 900 °C*  
204

205 According to our previous studies [15,34], the extensive volatilisation of Ca and  
206 Mg from char matrix during the gasification of Victorian brown coal in CO<sub>2</sub> at 900 °C  
207 in a fluidised-bed reactor took place because of the formation and aggregation of  
208 carbonates on char surface. Ca and Mg species were present as the carboxyl-bound

209 cations, and would retain their high dispersion during fast pyrolysis even at high  
210 temperature (up to 950 °C) [6,34]. Once the char was exposed to CO<sub>2</sub> at 900 °C, the  
211 well-dispersed alkali earth metallic species could be carbonated to form CaCO<sub>3</sub> and  
212 MgCO<sub>3</sub> on the char surface [34,35,36].



213



214

215 **Fig. 3.** Effects of acid washing on the XPS spectra of (a) survey scan and (b) high-resolution of O 1s  
216 peak of the char from the gasification of mallee wood at 900 °C in pure CO<sub>2</sub>.

217

218 This result was confirmed by the XPS analysis in this work. Fig. 3 shows the XPS  
219 spectra of the char from the gasification of mallee wood at 900 °C in pure CO<sub>2</sub>. The  
220 high-resolution O 1s spectrum showed a clear peak located at 535.0 eV, which is the

221 position for carbonate structures [37]. In order to clarify the nature of this band, the  
222 char was washed with 0.2 M hydrochloric acid to remove the carbonates as well as  
223 the AAEM species on char surface. It can be seen from the survey scan that almost  
224 all Ca and Mg species were removed from the char, and the band in the range of  
225 534.0-536.0 eV in the O 1s high-resolution spectrum disappeared after the acid-  
226 washing, indicating the formation of  $\text{CaCO}_3$  and  $\text{MgCO}_3$  during gasification in  $\text{CO}_2$  at  
227 900 °C. No clear carbonate peak can be seen in the O 1s high-resolution spectra of  
228 char from the gasification below 900 °C in pure  $\text{CO}_2$ .

229

#### 230 *4.3 Similarity in O/C ratio between surface and bulk analyses*

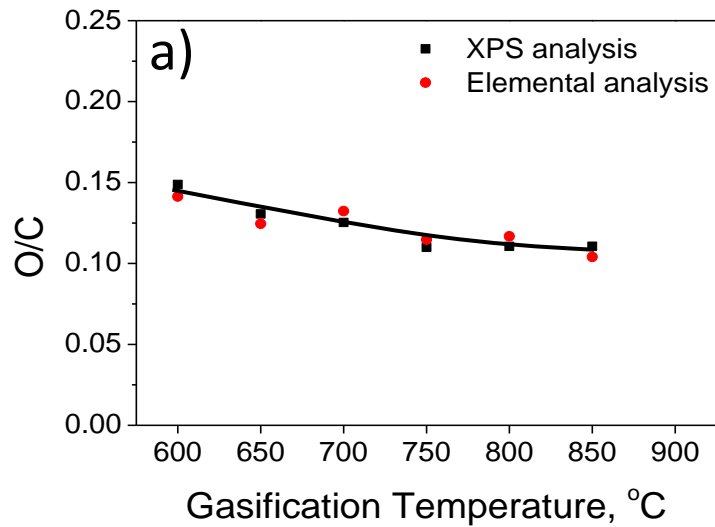
231

232 In order to identify whether there were some differences in the contents of carbon  
233 and oxygen between the char surface and the char matrix, the results from elemental  
234 analysis were compared with those from XPS analysis. The contents of carbon and  
235 oxygen in char from XPS analysis were obtained by the calculation of total peak  
236 intensity and the relative sensitivity factors of each element. Due to the inability to  
237 detect the H element through the XPS analysis, the O/C ratio of char during  
238 gasification was used to compare the difference between surface and bulk analyses.

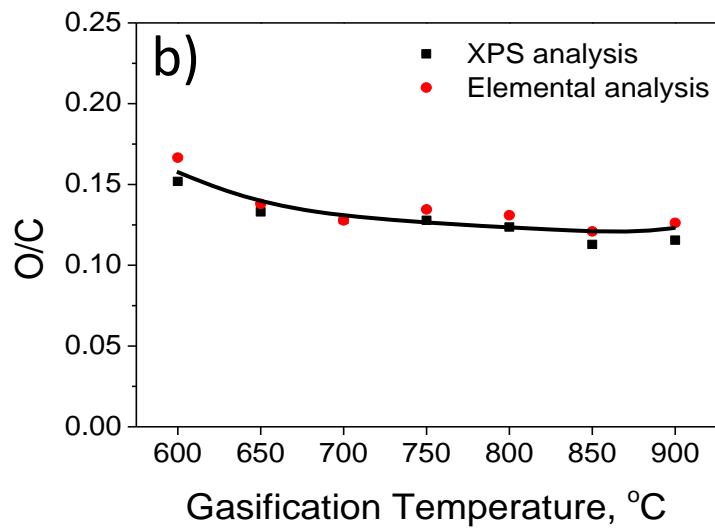
239 As is shown in Fig. 4, the O/C ratio of char obtained both from XPS and elemental  
240 analysis exhibited a decrease with the increasing gasification temperature, indicating  
241 the decline in the oxygen content of char during gasification at high temperature.  
242 More importantly, for a given temperature, the O/C ratios of char from XPS and  
243 elemental analysis were almost the same and the relative difference between these  
244 two analysis results was less than 6%, which means the whole char particle was  
245 chemically uniform and there was not much difference between the surface and char  
246 matrix. Although the XPS analysis cannot detect the H element in char, based on the

247 elemental analysis results, the content of H species in char was very little (less than  
248 2%). Therefore, the XPS analysis can still be used as a characterisation method to  
249 indicate the concentration of carbon and oxygen species of the whole char particles  
250 during gasification.

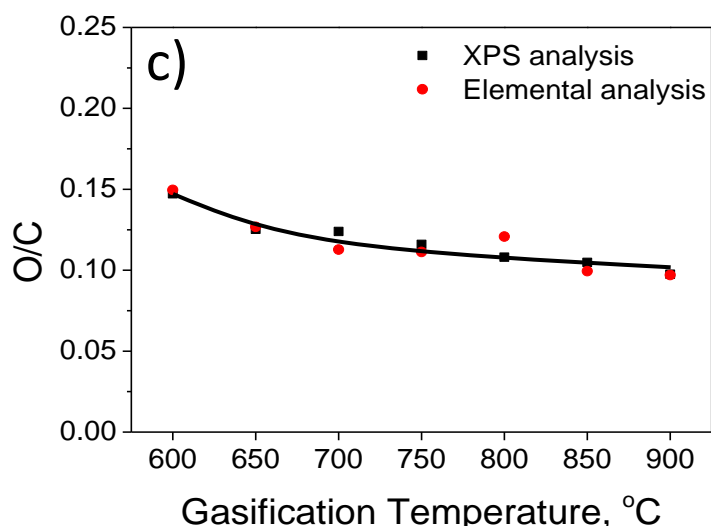
251



252



253



254

255 **Fig. 4.** The O/C ratios of chars as a function of gasification temperatures for mallee wood in (a) pure  
 256 CO<sub>2</sub>, (b) 15% H<sub>2</sub>O balanced with Ar and (c) 15% H<sub>2</sub> balanced with Ar.

257 *4.4 Relative distribution of chemical components in O 1s spectra*

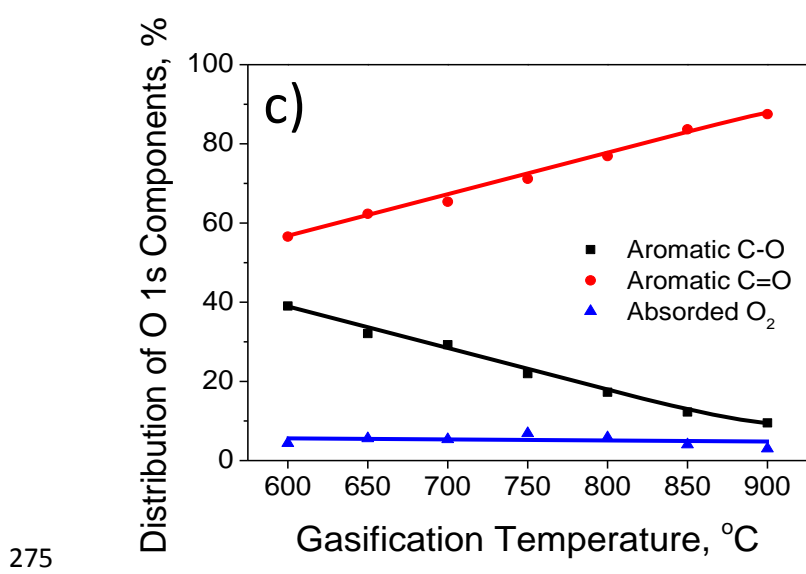
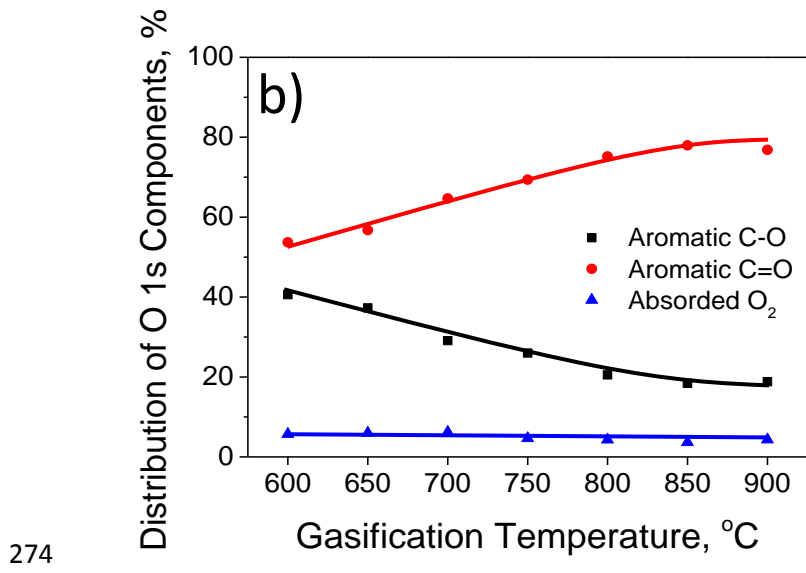
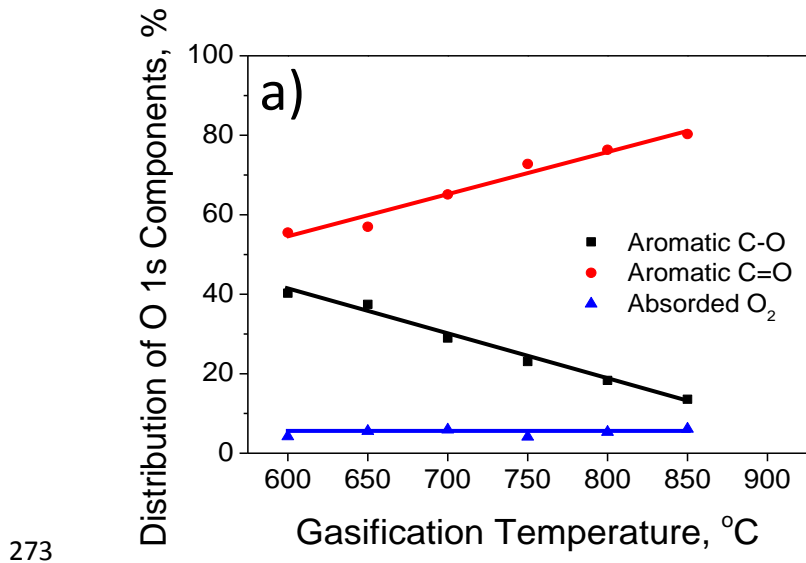
258

259 A clear trend for the changes in O-containing structure can be found through the  
 260 deconvolution of O 1s spectra of chars. Fig. 5 illustrates the relative distribution of O-  
 261 containing structures in O 1s high-resolution spectra. It can be seen that the  
 262 distribution of aromatic C-O structures in the O 1s spectra continuously decreased  
 263 with increasing gasification temperature, while an increasing trend was shown on the  
 264 distribution of aromatic C=O structures in the O 1s spectra with increasing  
 265 gasification temperature. The deconvolution result of O 1s spectra can only show the  
 266 relative content of O-containing structures, in order to identify the exact amount of O-  
 267 containing structures left in char during gasification, the absolute quantity of each  
 268 chemical component should be calculated, which will be discussed in the following  
 269 section.

270

271

272

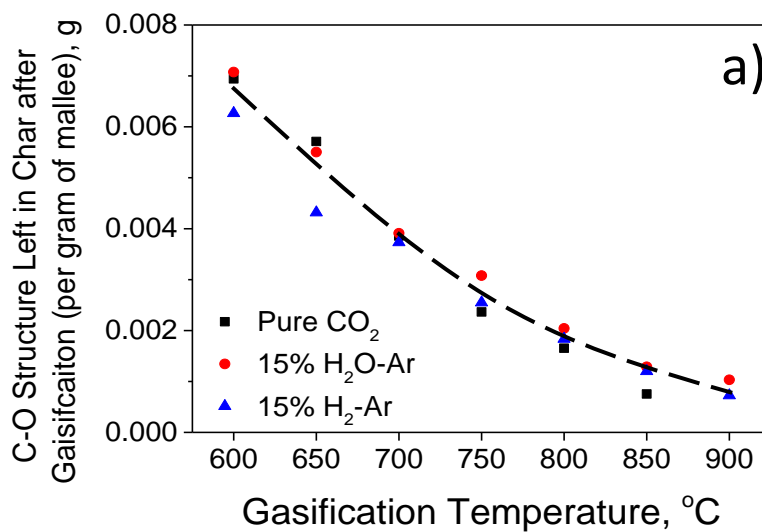


276 **Fig. 5.** Distribution of O-containing structure in O 1s spectra obtained by XPS analysis as a function of  
 277 gasification temperatures for mallee wood in (a) pure CO<sub>2</sub>, (b) 15% H<sub>2</sub>O balanced with Ar and (c) 15%  
 278 H<sub>2</sub> balanced with Ar.

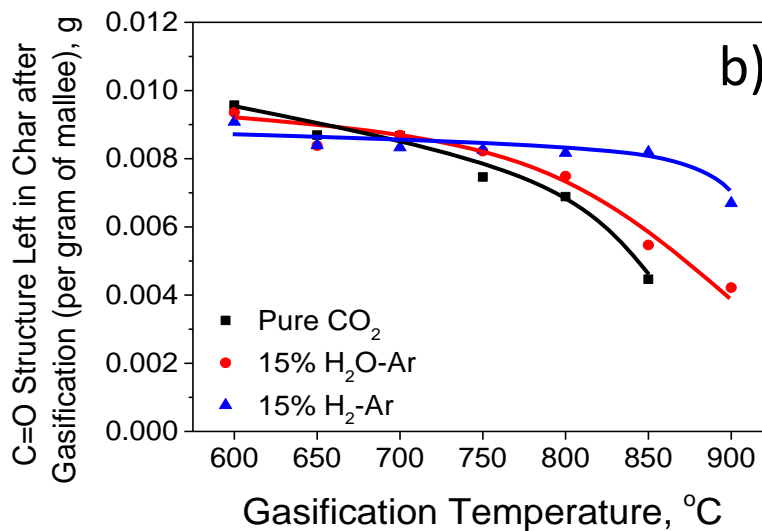
279 4.5 Absolute amount of oxygen species in char during gasification

280

281 The absolute amount refers to the amount of a particular type of XPS-derived O-  
282 containing structure in char based on an initial gram of biomass (before gasification  
283 at each temperature). The absolute amounts of O-containing structure in char  
284 obtained by the XPS calculation results and the char yield of mallee wood during  
285 gasification are illustrated in Fig. 6.



286



287

288 **Fig. 6.** Amount of (a) C-O structure and (b) C=O structure left in char after gasification based on per  
289 gram of mallee wood obtained by XPS analysis as a function of gasification temperatures.

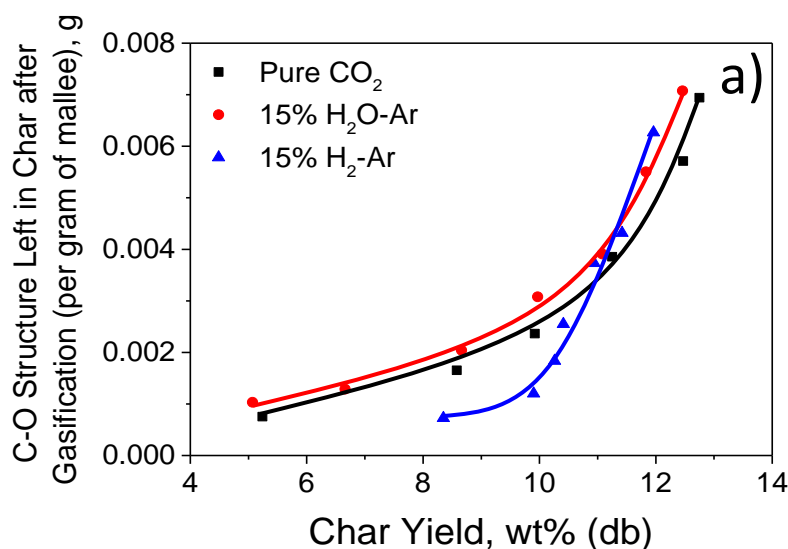
290

291 It can be seen that there was a drastic decrease in the aromatic C-O structures in  
292 char with increasing temperature for all three gasification atmospheres, indicating the  
293 high reactivity of aromatic C-O structures during gasification. In addition, a clear  
294 difference appeared for the amount of aromatic C=O structures left in char between  
295 gasification in H<sub>2</sub> atmosphere and the O-containing atmosphere (CO<sub>2</sub>, H<sub>2</sub>O). The  
296 amounts of C=O structures in char from the gasification in steam and in CO<sub>2</sub>  
297 continuously decreased with increasing temperature. However, such structure in  
298 chars from the gasification in H<sub>2</sub> was almost constant when the gasification  
299 temperature was below 900 °C. The char gasification in H<sub>2</sub> was quite slow and the  
300 loss of O-containing structure was mainly because of the enhanced thermal cracking,  
301 not the gasification reaction. Therefore, the chemical stability of the aromatic C=O  
302 structures made it more likely to survive during the thermal cracking and some  
303 aromatic C-O structures may transform to the more stable aromatic C=O structures,  
304 resulting in a steady amounts of aromatic C=O structures in char until 900 °C where  
305 the gasification become intensified. In contrast, for the char gasification in steam  
306 atmosphere and CO<sub>2</sub> atmosphere, the aromatic C=O structures would be  
307 continuously consumed by the gasifying agent, especially with increasing  
308 temperature and thus intensified gasification.

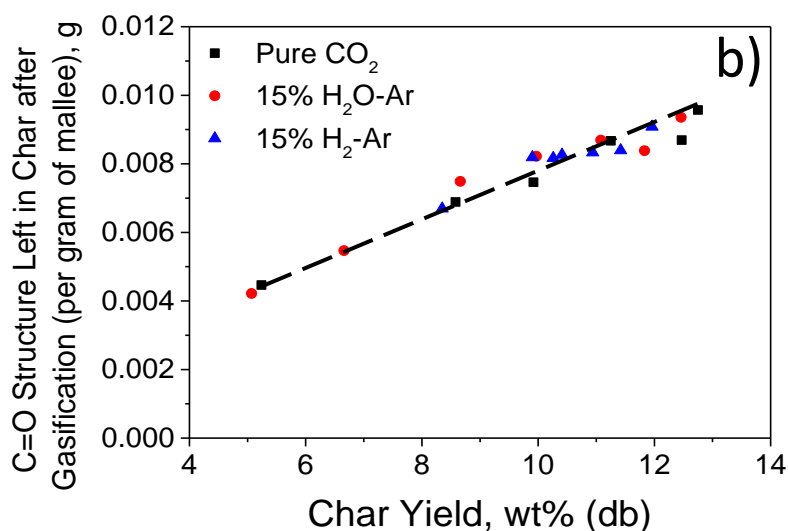
309 In order to clarify the changes in the O-containing structure with the progress of  
310 gasification, the absolute amounts of aromatic C-O structures and aromatic C=O  
311 structures in char as a function of char yield is shown in Fig. 7. It can be seen that,  
312 with the progress of gasification, the amounts of aromatic C-O structures of char  
313 from gasification in H<sub>2</sub> was significantly lower than that from gasification in the  
314 oxidising atmospheres, indicating that the C-O structures was easier to be consumed  
315 in the reducing atmospheres. In addition, as is shown in Fig. 7 (b), the amounts of



316 aromatic C=O structures decreased with decreasing char yield and not much  
 317 difference can be seen among the three atmospheres, which means that the  
 318 consumption of aromatic C=O structures was more likely to be proportional to the  
 319 progress of gasification both in the O-containing atmosphere and non-O-containing  
 320 atmosphere. Therefore, the steady amounts of aromatic C=O structures in char with  
 321 increasing temperature during the gasification in H<sub>2</sub> atmosphere was mainly due to  
 322 weak gasification reaction at that stage.



323



324

325 **Fig. 7.** Amounts of (a) C-O structure and (b) C=O structure left in char after gasification based on per  
 326 gram of mallee wood obtained by XPS analysis as a function of char yield.

327

328 *4.6 Oxygenation and de-oxygenation during char gasification*

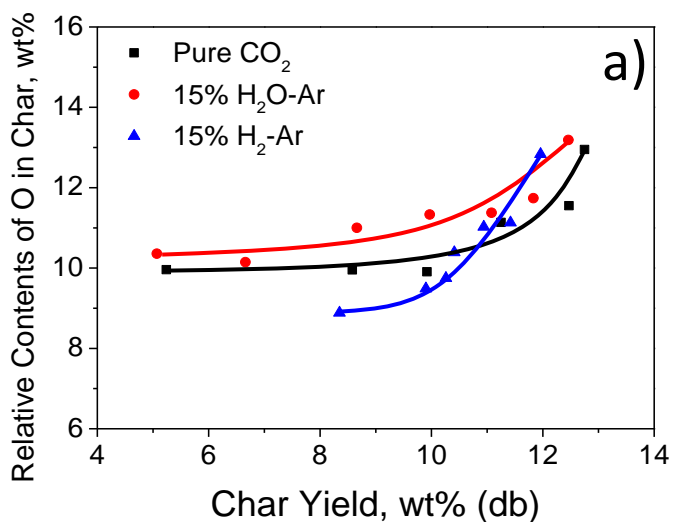
329

330 The gasification of low-rank fuels in O-containing atmospheres (e.g. H<sub>2</sub>O, CO<sub>2</sub>) is  
331 an oxygenation process based on our study of the total Raman intensity [4,9]. As  
332 mentioned above, the XPS analysis can also give a direct indication of the amount of  
333 O species in char during gasification, and it will involve all O species not just the O  
334 which have the resonance effect with the aromatic ring to which it is connected.

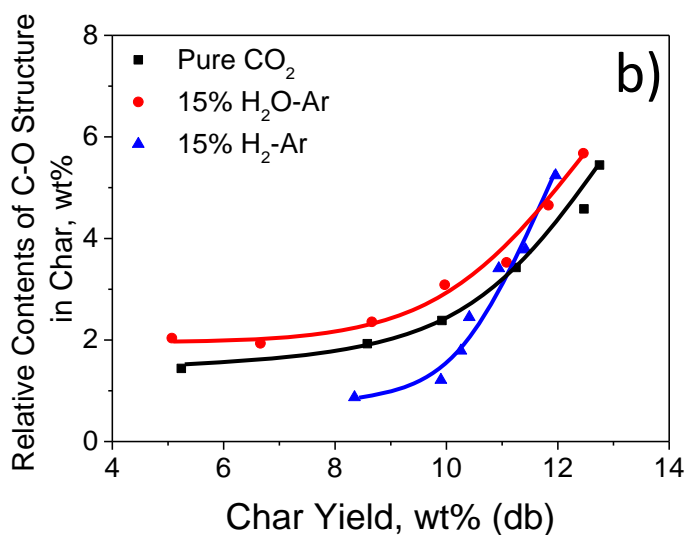
335 Fig. 8 illustrates the relative contents of O-containing structure in char with the  
336 progress of gasification. The relative contents refer to the contents of each chemical  
337 component in char based on per actual gram of biomass char (remaining after  
338 gasification). It can be seen that the relative contents of O species of char from  
339 gasification in the O-containing atmospheres were higher than that in the non-O-  
340 containing atmosphere with the process of gasification. Therefore, it is hypothesised  
341 that some O derived from the O-containing gasifying agent leads to the oxygenation  
342 of the aromatic ring system in terms of forming some intermediates such as C(CO),  
343 C(OH) and C(O) structures in the char matrix during gasification [9,38-41],  
344 contributing to the high contents of O species of char.

345

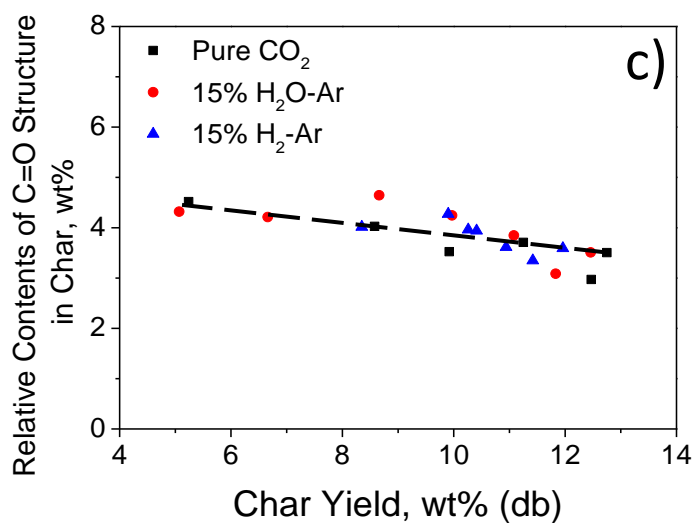
346



347



348



349

350 **Fig. 8.** Relative contents of (a) O species, (b) O with C-O structure and (c) O with C=O structure in  
 351 char obtained by XPS analysis as a function of char yield.

352 Further information can be obtained from the deconvolution result of the O 1s  
353 spectra. As is shown in Fig. 8 (b) and (c), The contents of aromatic C-O structure of  
354 char gasified in the O-containing atmosphere was much higher than that in the non-  
355 O-containing atmosphere with the process of gasification, while not much difference  
356 can be observed for the contents of aromatic C=O structure among the three  
357 atmospheres. All of these indicated that the captured O species from the O-  
358 containing gasifying agent were much likely bonded to the char matrix with C-O  
359 structure. Furthermore, considering the high gasification rate of char in steam  
360 atmosphere and in CO<sub>2</sub> atmosphere as well as our previous studies [4,9] which  
361 indicated that some kinds of O-containing structures in char were responsible for  
362 enhancing the char gasification rate, the continuously generated C-O structures in  
363 the O-containing atmosphere were most likely to be responsible for promoting the  
364 char gasification reactivity.

365

## 366 **5. Conclusions**

367

368 Australia mallee wood was gasified in a fluidised-bed reactor at 600-900 °C in O-  
369 containing atmosphere (pure CO<sub>2</sub>, 15% H<sub>2</sub>O-Ar) and non-O-containing atmosphere  
370 (15% H<sub>2</sub>-Ar). Our results revealed that the gasification rate of char in steam  
371 atmosphere and CO<sub>2</sub> atmosphere was much higher than that in H<sub>2</sub> atmosphere. For  
372 the gasification in CO<sub>2</sub> at 900 °C, CaCO<sub>3</sub> and MgCO<sub>3</sub> would form on char surface.  
373 The similar O/C ratio of char from XPS and elemental analysis indicated the  
374 chemical similarity between char surface and char matrix. In addition, the aromatic  
375 C-O structure in char was highly reactive so that it can be easily removed or broken  
376 down while the low reactivity of the aromatic C=O structure made it more likely to

377 survive during gasification compared with the aromatic C-O structure. The amount of  
378 aromatic C-O structure left in the char during gasification in non-O-containing  
379 atmosphere was lower than that in O-containing atmosphere, especially at low char  
380 yield. In contrast the consumption of aromatic C=O structure was proportional to the  
381 progress of gasification, regardless of the atmosphere. Moreover, the high contents  
382 of O species in chars with the progress of gasification in steam and in CO<sub>2</sub> confirmed  
383 the oxygenation of char gasified in the O-containing atmosphere. The newly formed  
384 C-O structure in char during the oxygenation was most likely to be responsible for  
385 the high gasification reactivity of char in the O-containing atmosphere.

386

### 387 **Acknowledgements**

388

389 This project received funding from the Australian Government through ARENA's  
390 Emerging Renewables Programs. This project was also supported by the Australian  
391 Research Council (DP110105514) and the Commonwealth of Australia under the  
392 Australia-China Science and Research Fund. The authors also acknowledge the use  
393 of equipment, scientific and technical assistance of the WA X-Ray Surface Analysis  
394 Facility, funded by the Australian Research Council LIEF grant LE120100026.

395

396

397

398

399

400

401

## References

- [1] C.-Z. Li, Special issue-gasification: A route to clean energy, *Process Saf. Environ. Prot.* 84 (2006) 407-408.
- [2] C.-Z. Li, Importance of volatile-char interactions during the pyrolysis and gasification of low-rank fuels – A review, *Fuel* 112 (2013) 609-623.
- [3] C.-Z. Li, Some recent advances in the understanding of the pyrolysis and gasification behaviour of Victorian brown coal, *Fuel* 86 (2007) 1664-1683.
- [4] H.-L. Tay, S. Kajitani, S. Wang, C.-Z. Li, A preliminary Raman spectroscopic perspective for the roles of catalysts during char gasification, *Fuel* 121 (2014) 165-172.
- [5] C.-Z. Li, C. Sathe, J.R. Kershaw, Y. Pang, Fates and roles of alkali and alkaline earth metals during the pyrolysis of a Victorian brown coal, *Fuel* 79 (2000) 427-438.
- [6] D.M. Quyn, H. Wu, S.P. Bhattacharya, C.-Z. Li, Volatilisation and catalytic effects of alkali and alkaline earth metallic species during the pyrolysis and gasification of Victorian brown coal. Part II. Effects of chemical form and valence, *Fuel* 81 (2002) 151-158.
- [7] T. Li, L. Zhang, L. Dong, S. Wang, Y. Song, L. Wu, C.-Z. Li, Effects of char chemical structure and AAEM retention in char during the gasification at 900° C on the changes in low-temperature char-O<sub>2</sub> reactivity for Collie sub-bituminous coal, *Fuel* 195 (2017) 253-259.
- [8] D. Lv, M. Xu, X. Liu, Z. Zhan, Z. Li, H. Yao, Effect of cellulose, lignin, alkali and alkaline earth metallic species on biomass pyrolysis and gasification, *Fuel Process. Technol.* 91 (2010) 903-909.

- [9] T. Li, L. Zhang, L. Dong, C.-Z. Li, Effects of gasification atmosphere and temperature on char structural evolution during the gasification of Collie sub-bituminous coal, *Fuel* 117 (2014) 1990-1995.
- [10] H.-L. Tay, S. Kajitani, S. Zhang, C.-Z. Li, Effects of gasifying agent on the evolution of char structure during the gasification of Victorian brown coal, *Fuel* 103 (2013) 22-28.
- [11] Y. Zhao, D. Feng, Y. Zhang, Y. Huang, S. Sun, Effect of pyrolysis temperature on char structure and chemical speciation of alkali and alkaline earth metallic species in biochar, *Fuel Process. Technol.* 141 (2016) 54-60.
- [12] L. Zhang, S. Kajitani, S. Umemoto, S. Wang, D. Quyn, Y. Song, T. Li, S. Zhang, L. Dong, C.-Z. Li, Changes in nascent char structure during the gasification of low-rank coals in CO<sub>2</sub>, *Fuel* 158 (2015) 711-718.
- [13] S. Zhang, Z. Min, H.-L. Tay, M. Asadullah, C.-Z. Li, Effects of volatile–char interactions on the evolution of char structure during the gasification of Victorian brown coal in steam, *Fuel* 90 (2011) 1529-1535.
- [14] X. Li, J.-i. Hayashi, C.-Z. Li, FT-Raman spectroscopic study of the evolution of char structure during the pyrolysis of a Victorian brown coal, *Fuel* 85 (2006) 1700-1707.
- [15] H.-L. Tay, C.-Z. Li, Changes in char reactivity and structure during the gasification of a Victorian brown coal: Comparison between gasification in O<sub>2</sub> and CO<sub>2</sub>, *Fuel Process. Technol.* 91 (2010) 800-804.
- [16] H.-L. Tay, S. Kajitani, S. Zhang, C.-Z. Li, Inhibiting and other effects of hydrogen during gasification: Further insights from FT-Raman spectroscopy, *Fuel* 116 (2014) 1-6.

- [17]X. Liu, Y. Zheng, Z. Liu, H. Ding, X. Huang, C. Zheng, Study on the evolution of the char structure during hydrogasification process using Raman spectroscopy, *Fuel* 157 (2015) 97-106.
- [18]S. Wang, T. Li, L. Wu, L. Zhang, L. Dong, X. Hu, C.-Z. Li, Second-order Raman spectroscopy of char during gasification, *Fuel Process. Technol.* 135 (2015) 105-111.
- [19]Y. Sekine, K. Ishikawa, E. Kikuchi, M. Matsukata, A. Akimoto, Reactivity and structural change of coal char during steam gasification, *Fuel* 85 (2006) 122-126.
- [20]X. Guo, H.-L. Tay, S. Zhang, C.-Z. Li, Changes in char structure during the gasification of a Victorian brown coal in steam and oxygen at 800 C, *Energy Fuels* 22 (2008) 4034-4038.
- [21]D.L. Perry, A. Grint, Application of XPS to coal characterization, *Fuel* 62 (1983) 1024-1033.
- [22]S.G. Chen, R.T. Yang, F. Kapteijn, J.A. Moulijn, A new surface oxygen complex on carbon: toward a unified mechanism for carbon gasification reactions, *Ind. Eng. Chem. Res.* 32 (1993) 2835-2840.
- [23]S.D. Gardner, C.S.K. Singamsetty, G.L. Booth, G.-R. He, C.U. Pittman, Surface characterization of carbon fibers using angle-resolved XPS and ISS, *Carbon* 33 (1995) 587-595.
- [24]F. Marquez-Montesinos, T. Cordero, J. Rodriguez-Mirasol, J.J. Rodriguez, CO<sub>2</sub> and steam gasification of a grapefruit skin char, *Fuel* 81 (2002) 423-429.
- [25]A.R. Gonzalez-Elipe, A. Martinez-Alonso, J.M.D. Tascon, XPS characterization of coal surfaces: study of aerial oxidation of brown coals, *Surf. Interface Anal.* 12 (1988) 565-571.



- [26] Y. Qiao, S. Chen, Y. Liu, H. Sun, S. Jia, J. Shi, C.M. Pedersen, Y. Wang, X. Hou, Pyrolysis of chitin biomass: TG-MS analysis and solid char residue characterization, *Carbohydr. Polym.* 133 (2015) 163-170.
- [27] G. Levi, O. Senneca, M. Causa, P. Salatino, P. Lacovig, S. Lizzit, Probing the chemical nature of surface oxides during coal char oxidation by high-resolution XPS, *Carbon* 90 (2015) 181-196.
- [28] A.M. Puziy, O.I. Poddubnaya, R.P. Socha, J. Gurgul, M. Wisniewski, XPS and NMR studies of phosphoric acid activated carbons, *Carbon* 46 (2008) 2113-2123.
- [29] Wang S, Evolution of char structure and reactivity during gasification, dissertation, Curtin University, 2016.
- [30] W. Xia, J. Yang, C. Liang, Investigation of changes in surface properties of bituminous coal during natural weathering processes by XPS and SEM, *Appl. Surf. Sci.* 293 (2014) 293-298.
- [31] D. Briggs, G. Beamson, XPS studies of the oxygen 1s and 2s levels in a wide range of functional polymers, *Anal. Chem.* 65 (1993) 1517-1523.
- [32] E. Desimoni, G.I. Casella, A. Morone, A.M. Salvi, XPS determination of oxygen-containing functional groups on carbon-fibre surfaces and the cleaning of these surfaces, *Surf. Interface Anal.* 15 (1990) 627-634.
- [33] S. Glenis, M. Benz, E. LeGoff, J.L. Schindler, C.R. Kannewurf, M.G. Kanatzidis, Polyfuran: a new synthetic approach and electronic properties, *J. Am. Chem. Soc.* 115 (1993) 12519-12525.
- [34] D.M. Quyn, J.-i. Hayashi, C.-Z. Li, Volatilisation of alkali and alkaline earth metallic species during the gasification of a Victorian brown coal in CO<sub>2</sub>, *Fuel Process. Technol.* 86 (2005) 1241-1251.

- [35] C.S.M. Lecea, M. Almela-Alarcon, A. Linares-Solano, Calcium-catalysed carbon gasification in CO<sub>2</sub> and steam, *Fuel* 69 (1990) 21-27.
- [36] M.B. Cerfontain, J.A. Moulijn, The interaction of CO<sub>2</sub> and CO with an alkali carbonate carbon system studied by in-situ Fourier Transform infrared spectroscopy, *Fuel* 65 (1986) 1349-1355.
- [37] M. Ni, B.D. Ratner, Differentiating calcium carbonate polymorphs by surface analysis techniques – an XPS and TOF-SIMS study, *Surf. Interface Anal.* 40 (2008) 1356-1361.
- [38] M. Jiang, J. Hu, J. Wang, Calcium-promoted catalytic activity of potassium carbonate for steam gasification of coal char: effect of hydrothermal pretreatment, *Fuel* 109 (2013) 14-20.
- [39] T.-W. Kwon, S.D. Kim, D.P.C. Fung, Reaction kinetics of char-CO<sub>2</sub> gasification, *Fuel* 67 (1988) 530-535.
- [40] K.J. Huttinger, Mechanism of water vapor gasification at high hydrogen levels, *Carbon* 26 (1988) 79-87.
- [41] G. Hermann, K.J. Huttinger, Mechanism of water vapour gasification of carbon – A new model, *Carbon* 24 (1986) 705-713.